Peer-reviewed version available at Nanomaterials 2019, 9, 1348; doi:10.3390/nano9101348

Article

Multi-Purpose Nanovoid Array Plasmonic Sensor Produced by Direct Laser Patterning

Dmitrii V. Pavlov[1,2], Alexey Yu. Zhizhchenko[1,2], Mitsuhiro Honda[3], Masahito Yamanaka[4], Oleg B. Vitrik[1,2], Sergey A. Kulinich[1,5], Saulius Juodkazis[6,7], Sergey I. Kudryashov[2,8,9], and Aleksandr Kuchmizhak[1,2,*]

1 Far Eastern Federal University, Vladivostok 690041, Russia
2 Institute of Automation and Control Processes, Far Eastern Branch, Russian Academy of Sciences, Vladivostok 690091, Russia
3 Graduate School of Engineering, Nagoya Institute of Technology, Nagoya 466-8555, Japan
4 Graduate School of Engineering, Nagoya University, Nagoya 464-8603, Japan
5 Research Institute of Science and Technology, Tokai University, Hiratsuka, Kanagawa 259-1292, Japan
6 Swinburne University of Technology, Hawthorn 3122 VIC, Australia
7 Melbourne Centre for Nanofabrication, ANFF, Clayton 3168 VIC, Australia
8 Lebedev Physical Institute, Russian Academy of Sciences, Moscow 119991, Russia
9 National Research Nuclear University MEPhI, Moscow 115409, Russia
* Correspondence: alex.iacp.dvo@mail.ru

Abstract: We demonstrate a multi-purpose plasmonic sensor based on nanovoid array fabricated *via* inexpensive and highly reproducible direct femtosecond laser patterning of thin glass-supported Au films. The proposed nanovoid array exhibits near-IR surface plasmon (SP) resonances, which can be excited under normal incidence and optimised for specific application by tailoring array periodicity as well as nanovoid geometric shape. Fabricated SP sensor offers competitive sensitivity of ≈1600 nm/RIU at a figure of merit of 12 in bulk refractive index tests, as well as allows for identification of gases and ultra-thin analyte layers making the sensor particularly useful for common bioassay experiments. Moreover, isolated nanovoids support strong electromagnetic field enhancement at lattice SP resonance wavelength, allowing for label-free molecular identification via surface-enhanced vibration spectroscopy.

Keywords: direct femtosecond laser printing; nanovoid arrays; plasmonic sensors; refractive index and gas sensing

1. Introduction

Resonant oscillation of free electron plasma, surface plasmons (SPs), supported by either noble-metal nanostructures or metal-dielectric interfaces upon their excitation with visible or near-IR light is a key effect behind realisation of state-of-the-art chemo- and biosensors. SPs give rise to highly enhanced and localised electromagnetic (EM) fields which strongly react on any perturbation of the surroundings [1], permitting to detect, for example, local changes of the refractive index (RI) caused by molecular binding, chemical reactions [2,3] and gases as well as to boost characteristic IR absorption and Raman scattering of the surrounding molecules [4,5]. These features made plasmonic-based label-free sensors extremely popular and valuable tools for medical diagnostics, environmental monitoring, food safety and security [6].

Alongside with the significant progress in the field of SP sensors made in the past several decades, there is still a need for facile and inexpensive technologies allowing fabrication of high-quality sensors having competitive characteristics and merging different modalities in a single sensor element [2,7,8]. Utilisation of well-developed top-down approaches as electron- or ion-beam milling allows fabrication

of plasmon-active nanostructures and related SP sensors at nanometer-scale precision. However, these approaches become extremely time-and money-consuming for fabrication of mm-scale sensors. Also noteworthy is that single-use sensors are required for many applications limiting applicability of mentioned methods for mass production. Various chemical synthesis methods are well adopted for mass production of only disordered plasmonic nanostructures of a certain size and shape [9,10]. Additional preliminary processing steps are required to arrange the synthesized nanostructures into the ordered arrays, which can support low-loss lattice-type SP resonances. Such geometrical resonances coming from periodical arrangement of coupled plasmonic nanoantennas can be characterized by higher quality factor which is indeed favorable for various sensing applications.

Alternatively, utilisation of direct pulsed laser processing of plasmon-active materials (e.g. noble metal films) can be considered as a promising route for high-performing flexible and inexpensive mass production of various plasmonic nanostructures and their arrangements [11–13]. However, interaction of ultra-short femtosecond (fs) laser pulses with the metal films is typically associated with the ejection and redepositon of multiple ablative nanoparticles precluding clean and highly reproducible printing of nanostructure arrays supporting spectrally narrow SP resonances. The issue becomes even more challenging when ultra-fast direct laser printing is applied to fabricate nanostructure arrangements separated by micron scale distances to bring the collective resonance to the near IR spectral range. Presence of transparency windows of aqueous solutions [14] as well as strong electromagnetic field localization supported by plasmonic nanostructures [15] make this spectral range extremely promising for multi-purpose SP sensor realization.

In this paper, we demonstrate a multi-purpose SP biosensing platform based on periodically arranged nanovoids produced via inexpensive direct ablation-free femtosecond (fs) laser patterning of thin glass-supported Au films. Such nanovoid arrays support near-IR lattice-type SP resonances, which can be tailored to enable specific sensing modality by adjusting both nanovoid geometric shape and arrangement. Fabricated SP sensor offers competitive sensitivity of ≈1600 nm/RIU at a figure of merit of 12 in typical bulk refractive index test experiments, as well as allows identification of gases and ultra-thin superstrate layers making the sensor particularly useful for common bioassay experiments. Moreover, the isolated nanovoids support strong electromagnetic field enhancement at lattice SP resonance wavelength, allowing label-free molecular identification via surface-enhanced vibration spectroscopy.

2. Results

SP sensors were fabricated *via* direct fs-laser ablation-free nanopatterning of the 50-nm thick Au film covering silica glass substrate according to the procedure described elsewhere [16]. Briefly, the 200-fs second-harmonic (515 nm wavelength) laser pulses generated at a 200 KHz repetition rate by a regeneratively amplified Yb:KGW laser system (Pharos, Light Conversion) were focused with a dry microscope lens having the numerical aperture of 0.5 to achieve the 1-μm-diameter Gaussian-shaped spot on the metal film surface. Within a certain range of applied energies, each laser pulse melts locally a small section of the irradiated Au film. Molten section of the film has weaker adhesion comparing to surrounding solid parts, resulting in its detachment from the supporting glass substrate via acoustic relaxation of thermal-generated stress and subsequent resolidification in the form of a parabolic nanovoid. Detailed description of the underlying physical process behind the formation of nanovoids can be found elsewhere [17,18]. The sample was translated by a 3-axis nanopositioning system (Aerotech GmBH) to fabricate rectangular nanovoid arrays by a single-shot single-structure approach (Fig. 1a).

Ordered arrays of the laser-printed nanovoids demonstrate a pronounced dip in the near-IR reflection spectrum further referred to as first-order lattice plasmonic resonance (FLPR), which can be explained in terms of an excitation and interference of SP waves [16,19]. In particular, periodically arrange nanovoids with their smooth surface morphology provide efficient coupling of the normally incident IR radiation to the SP waves. Being simultaneously launched by these identical laser-printed

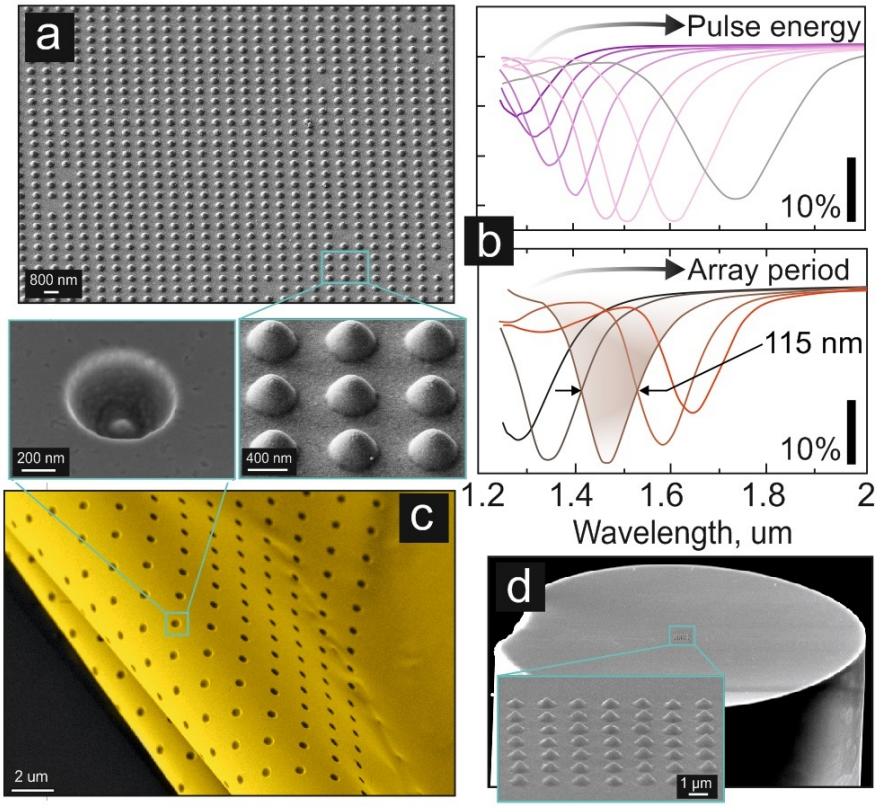

Figure 1. Nanovoid array SP sensor produced via direct ablation-free laser printing. (a) Side-view (view angle of 45°) SEM images of a nanovoid array printed at 0.8 μm lattice periodicity (top); a close-up images of the isolated nanovoid backside and a close-up view of an array. (b) FTIR reflection spectra measured from the nanovoid arrays printed at fixed periodicity of 1.2 μm and various pulse energy from 1 to 2.1 nJ (top); and at fixed pulse energy of 1.2 nJ and various periodicity from 0.8 to 1.2 μm (bottom). (c) SEM image (view angle of 78°) of the nanovoid array (the inset) produced at the end-face of a standard 125-μm diameter single-mode optical fibre. (d) SEM images showing the back-side of the Au film patterned by the nanovoid arrays.

nanostructures, SPs waves travel along nanovoid curvy surface and further along the smooth Au film surface interfering in between. In this respect, spectral position of the FLPR resonance is defined by an "effective" lattice period, p_{eff}, which depends on both the actual array periodicity p as well as the geometric shape of the laser-printed nanostructures (nanovoids). The latter can be tailored by varying the incident pulse energy E (per single spot) [16]. These features provide remarkable flexibility for on-demand optimisation of the optical properties of the nanovoid arrays. In Fig. 1b, two series of FTIR reflection spectra of the nanovoid arrays illustrate tunability of the FLPR spectral position *via* tuning the geometry of nanovoids within the array printed at fixed period $p = 1.1\,\mu$m and variable pulse energy E (top panel, Fig. 1b) and at fixed pulse energy of $E = 1.3$ nJ (nanovoid geometry) and array periodicity p ranging from 0.8 to 1.2 μm (bottom panel, Fig. 1b).

In general, the described simple inexpensive and ablation-free fs-laser nanopatterning allows to produce high-quality nanovoid arrays, which support geometry-dependent tunable near-IR SP lattice resonances with a Q-factor up to 13 (full width at half maximum of FLPR $\approx$ 115 nm; Fig. 1b, bottom panel). Taking into account high short-term pulse-to-pulse stability ($\approx$0.05 %) of the laser system providing nearly perfect replication of the nanovoid shape, the resulting reproducibility of the FLPR resonance position was always within $\pm$50 nm as it was measured for multiple samples fabricated at fixed values of E and p.

Noteworthy, multi-beam interference lithography as well as various DOE-mediated beam multiplexing techniques can be adopted to achieve extremely fast patterning of the Au films with the

nanovoid structures at a printing rate up to 10^6 elements per second [19–24]. Notably, the developed ablation-free fabrication protocol does not perturb integrity of the Au film and its basic mechanical properties. The produced nanovoid array element is as robust as the initial unpatterned Au film on a substrate and is more durable than lithographically produced plasmonic nanoantenna array. Moreover, nanovoid arrays can be directly patterned on any smooth surface of a thin noble-metal film covering heat-insulating substrate (e.g. glass or silicon). For example, such structure can be produced within smooth microfluidic channels or even at the end-face of the optical fibre (Fig. 1c). Moreover, using a standard procedure developed for 2D materials, the produced metal film patterned with the nanovoid arrays can be pilled off from the supporting glass (or silicon) substrate and transferred in the form of a membrane to another surface, including flexible polymers. Such transfer does not cause any deformation of the nanovoids (Fig. 1d), which gives extra versatility for design and fabrication of functional sensing devices.

Spectral position of any plasmonic mode supported by a dielectric-metal interface is known to react on the RI of the dielectric media [1]. This feature makes the proposed laser-printed nanovoid arrays supporting the lattice-type FLPR with rather high Q-factor in the near-IR spectral range potentially applicable for biosensing applications based on measurements of bulk and local variations of the RI [6]. To evaluate the performance of the produced sensors, we have carried three lines of experiments: (1) sensing bulk liquid filled above the arrays; (2) sensing thin films deposited on top of the arrays; and (3) measuring sensitivity to vapours and gases.

First, we assessed the sensitivity of the resonance of the nanovoid array to variation of the bulk RI of the surrounding dielectric medium (superstrate). The experiments were performed by measuring the FTIR reflection from a fabricated nanovoid array with FLPR at around 1.7 μm, with various liquids filled in a home-built measuring cell having an IR-transparent quartz glass output window. We have used water H_2O, isopropanol C_3H_7OH, toluene C_7H_8, as well as water/isopropanol mixtures in various proportions, thereby achieving a set of RI in the range from 1 (no filling) to 1.475 (toluene) [14,25,26]. The corresponding FTIR reflection spectra (Fig. 2a) demonstrate a clear redshift of the FLPR with an increase of the refractive index n of the superstrate medium. The dependence of the experimentally measured relative spectral shift $\Delta = \lambda - \lambda_0$ of this lattice resonance on the superstrate bulk RI n shown in Fig.2b (markers) reveals its almost linear behaviour and demonstrates the relative sensitivity of ≈ 1600 nm/RIU with the figure-of-merit of about 12. Such competitive characteristics are good enough to detect the changes of the refractive index of the bulk dielectric superstrate as small as 10^{-5}, taking into account the spectral resolution of the common FTIR spectrometers [27]. The trialled sensory elements withstood at least 50 measurement cycles in various liquids without changing the wavelength of the main lattice resonance in air, which confirms good mechanical stability and robustness of the isolated nanostructures within the array. Good mechanical stability of the nanovoids being combined with excellent chemical stability of the Au material to various cleaning chemicals make the proposed sensor fully reusable.

In view of the nature of the FLPR at the patterned dielectric-metal interface, outlined above (see also [16,19]), the plasmon resonance is observed when the incident free-space wavelength λ_0 satisfies

$$p_{\text{eff}} = \lambda_{\text{SP}} = \lambda_0 \sqrt{\frac{1}{\varepsilon_{\text{m}}} + \frac{1}{\varepsilon_{\text{s}}}}$$

making is directly sensitive to the permittivity ε_{s} of the environment. Given that the permittivity of gold $\varepsilon_{\text{m}} \gg \varepsilon_{\text{s}}$ in the IR range, the resulting dependence of the resonance on the refractive index n_{s} is approximately linear,

$$\lambda_0 \approx p_{\text{eff}} n_{\text{s}}.$$

The observed linear slope of $\Delta(n)$ dependence (blue dotted line in Fig. 2b) agrees well with the theoretically predicted expectation (red dashed line in Fig. 2b). A small deviation from the theory might be explained by an incomplete wetting of the metal surface with the superimposed liquids.

Preprints (www.preprints.org) | NOT PEER-REVIEWED | Posted: 29 August 2019 doi:10.20944/preprints201908.0307.v1

Peer-reviewed version available at Nanomaterials 2019, 9, 1348; doi:10.3390/nano9101348

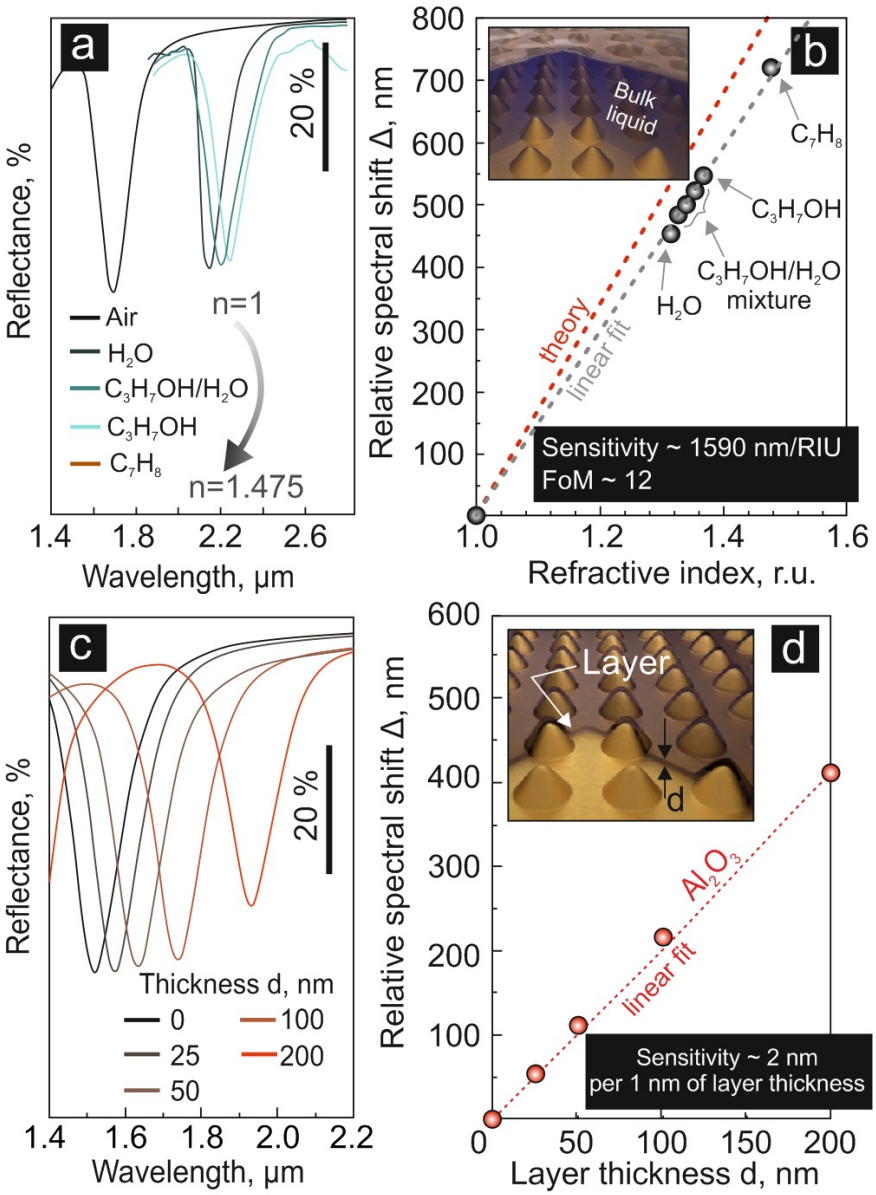

Figure 2. Performance of FLPR nanovoid array sensor for detection of bulk and local refractive index changes. (a) FTIR reflection spectra showing the spectral position of the FLPR of the nanovoid array immersed in different liquids having the refractive indices ranging from 1 to 1.475 (for toluene, the reflection spectrum is provided in Fig. 3a). (b) Measured (markers) and calculated (red dashed line) relative spectral shift of the FLPR depending on the refractive index of the superstrate medium. (c) FTIR spectra of the nanovoid array covered by a thin alumina layer of variable thickness d. (d) Measured (markers) and calculated (dashed curve) relative spectral shift of the lattice resonance as a function of the thickness d of the alumina capping layer. The insets in panels b and d illustrate schematics of the experiments.

Second, we have tested the performance of the nanovoid array with respect to a deposition of nm-thick layers, which is a rough imitation for chemical binding of analytes. Using the e-beam deposition we have imposed a series of alumina (Al_2O_3) layers ($n_s = 1.742 \pm 0.005$ at 1.5–2 μm wavelength [28,29]) of calibrated thickness d up to 200 nm above the nanovoid arrays. The resulting thickness of the deposited layers was verified using the atomic-force microscopy as well as, for thicker layers, zero-order optical transmission/reflection measurements. As expected for optically

Preprints (www.preprints.org) | NOT PEER-REVIEWED | Posted: 29 August 2019 doi:10.20944/preprints201908.0307.v1

Peer-reviewed version available at Nanomaterials 2019, 9, 1348; doi:10.3390/nano9101348

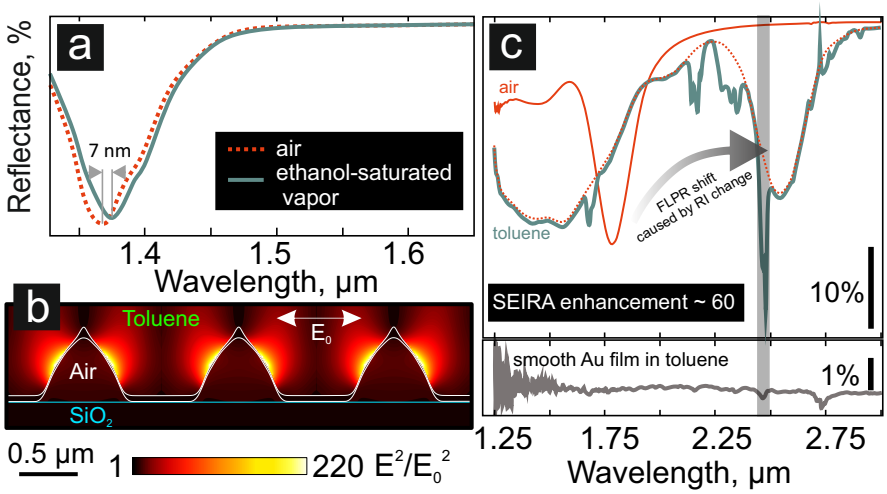

Figure 3. Various applications of the FLPR sensors. (a) Spectral response of the nanovoid array SP sensor caused by injection of saturated ethanol vapour. (b) Squared normalised EM-field amplitude E^2/E_0^2 calculated near the surface of nanovoid array immersed in toluene, upon its excitation from the top by a linearly polarised source at 2.5 μm wavelength. (c) FTIR reflection spectra of the nanovoid array in air and under the toluene liquid layer. Dashed curve provides the contribution of the nanovoid array to the reflection spectrum, if taken without the absorption of toluene. The bottom panel shows FTIR reflection from the smooth Au film surface covered by toluene obtained under the same conditions.

thin superstrates, the recorded FLPR spectra demonstrate an approximately linear redshift Δ with an increase of the layer thickness d (Fig. 2 c,d). The presented data imply a sensitivity of $\approx$ 2 nm spectral shift per 1-nm layer thickness, which would allow for detection of sub-nm capping layers with conventional spectrometers (typically having 1 nm spectral resolution).

Noteworthy, for the layer thickness above 200 nm, the deviation between theoretical estimations and experimental results increases gradually (not shown here). This behaviour could be explained in terms of complicated interaction of various waveguide and SPP modes supported by the air-dielectric-metal system having an optically "thick" dielectric layer. The detailed analysis of the modes supported by such system can be potentially performed using numerical methods. Nevertheless, the case of the thick capping layer is less relevant from the practical point of view, while such studies indeed fall outside the scope of this paper. We plan to analyse these features in a future study.

Third, we have evaluated the performance of the proposed nanovoid array SP sensor towards the detection of gaseous environments. To this end, we have exposed the sample to ethanol-saturated air in a home-made gas chamber setup previously described elsewhere [30]. The gas concentration in the chamber was calculated to be 7.8 vol.% (or $\approx$160 mg/L) according to saturated vapour pressure, which is equals to 59.0 mmHg at 25 ^{o}C. As shown in Fig. 3a, such an exposure led to a detectable spectral shift of the FLPR by $\approx$7 nm via the corresponding change of the local RI of the surroundings. The FLPR spectral shift appears to be caused by a two-fold effect, with a nanometre-thick ethanol layer absorbed onto the sensor surface as well as increase of the bulk refractive index caused by gas presence. Importantly, the spectral shift is reversible when the chamber is refilled by air.

Finally, we note that the nanovoids can produce strongly enhanced and localised electromagnetic (EM) near-fields which penetrate into the superstrate. We have assessed this feature with the help of 3D FDTD numerical simulations performed using a commercial software package (Lumerical Solutions). SEM images of the focused ion beam cuts previously reported in Ref. [17] were utilised to model the 3D shape of nanovoids. Nanovoid array placed below semi-infinite layer of toluene was illuminated from the top with a linearly polarised plane-wave source at the wavelength corresponding to the FLPR resonance in this environment. 3D simulations were performed at ultrafine 1 nm^3 mesh considering periodic boundary conditions in both horizontal directions and perfectly matched layers as the boundary conditions limiting the vertical directions of the computation volume. Fig. 3b shows

normalised squared EM-field amplitude E^2/E_0^2 calculated for the nanovoid array in toluene at 2.5 μm incident wavelength, demonstrating up to 220-fold enhancement. This feature makes the nanovoid arrays with tailored plasmonic response potentially applicable for label-free identification of molecular species based on surface-enhanced IR absorption (SEIRA). FTIR reflection spectrum of the nanovoid array covered with ≈ 10 μm-thick layer of toluene (Fig. 3c, top panel) demonstrates an enhancement of several IR overtones of toluene, spectrally matching the FLPR of the array. In comparison to the same spectrum obtained from a smooth Au film (Fig. 3c, bottom panel), this makes for a SEIRA enhancement factor of ≈ 60 for the certain IR band overtone of toluene.

3. Conclusions

In summary, in this paper we have demonstrated that laser-printed periodically arranged nanovoid arrays offer a novel flexible multi-purpose sensing platform, potentially useful for bioassay studies and various chemo- and biosensing applications. Specifically, the FLPR of the nanovoid array is highly sensitive to both local and bulk RI changes of the superstrate. In addition, we have also indicated the applicability of such arrays for gas and SEIRA-based molecular sensing.

Remarkably, even at moderate focusing conditions (NA=0.5), fs-laser printing is capable of producing nanovoid arrays at sub-μm periodicity [31,32]. This will bring the FLPR spectral position to below 1 μm, where inexpensive and high-resolution spectrometers with Si-based detectors can be implemented. Moreover, as shown in previous studies, isolated nanovoids support tunable geometry-dependent localised plasmon resonances (LPRs) in the visible spectral range [31]. This makes it possible to utilise isolated nanovoids for molecule identification based on surface-enhanced Raman scattering as well as LPR-based sensing, which is known to provide a better spatial resolution and better sensitivity to local RI variations, within the only sensor element. Also noteworthy is that the resonant nanovoid arrays can be produced on the surface of other noble metal films (as Ag, Cu, Pd and Pt, [16]) as well as their alloys providing flexibility in term of tailoring their physical and chemical properties. This feature is expected to further extend the application range of the proposed SP sensors, for example, to realized hydrogen gas sensors [33,34], etc.

Overall, a wide flexibility of the fabrication process with respect to nanovoid geometrical shape and array periods makes it possible to suitably adjust the spectral range of the proposed sensing platform. Given the high speed and cost-efficiency of the underlying liquid-free chemical-free process, our design provides an important technological platform for realistic applications and devices for medical diagnostics, environmental monitoring, food safety and security.

Author Contributions: D.V.P. performed sample preparation and laser fabrication experiments as well as made FTIR characterization and RI sensing, A.Yu.Zh. made FDTD calculations, M.H. and M.Y. carried out gas sensing experiments, O.B.V., S.A.K., S.J. and S.I.K. helped with experiment design, analyzed the data and participated in manuscript preparation. A.A.K. supervised the project and wrote manuscript.

Funding: This work was supported by Russian Science Foundation (grant no. 19-12-10165)

Acknowledgments: Authors are thankful to Prof. M. Lapine for helpful discussion and careful reading of the manuscript.

Conflicts of Interest: The authors declare no conflict of interest.

1. Maier, S.A. *Plasmonics: fundamentals and applications*; Springer Science & Business Media, 2007.
2. Cetin, A.; Yanik, A.A.; Yilmaz, C.; Somu, S.; Busnaina, A.; Altug, H. Monopole antenna arrays for optical trapping, spectroscopy, and sensing. *Applied Physics Letters* **2011**, *98*, 111110.
3. Špačková, B.; Wrobel, P.; Bocková, M.; Homola, J. Optical biosensors based on plasmonic nanostructures: a review. *Proceedings of the IEEE* **2016**, *104*, 2380–2408.
4. Neubrech, F.; Pucci, A.; Cornelius, T.W.; Karim, S.; García-Etxarri, A.; Aizpurua, J. Resonant plasmonic and vibrational coupling in a tailored nanoantenna for infrared detection. *Physical review letters* **2008**, *101*, 157403.

5. Neubrech, F.; Huck, C.; Weber, K.; Pucci, A.; Giessen, H. Surface-enhanced infrared spectroscopy using resonant nanoantennas. *Chemical reviews* **2017**, *117*, 5110–5145.
6. Homola, J.; Yee, S.S.; Gauglitz, G. Surface plasmon resonance sensors. *Sensors and Actuators B: Chemical* **1999**, *54*, 3–15.
7. Masson, J.F.; Murray-Méthot, M.P.; Live, L.S. Nanohole arrays in chemical analysis: manufacturing methods and applications. *Analyst* **2010**, *135*, 1483–1489.
8. Jones, M.R.; Osberg, K.D.; Macfarlane, R.J.; Langille, M.R.; Mirkin, C.A. Templated techniques for the synthesis and assembly of plasmonic nanostructures. *Chemical reviews* **2011**, *111*, 3736–3827.
9. Xia, Y.; Xiong, Y.; Lim, B.; Skrabalak, S.E. Shape-controlled synthesis of metal nanocrystals: simple chemistry meets complex physics? *Angewandte Chemie International Edition* **2009**, *48*, 60–103.
10. Rycenga, M.; Cobley, C.M.; Zeng, J.; Li, W.; Moran, C.H.; Zhang, Q.; Qin, D.; Xia, Y. Controlling the synthesis and assembly of silver nanostructures for plasmonic applications. *Chemical reviews* **2011**, *111*, 3669–3712.
11. Malinauskas, M.; Žukauskas, A.; Hasegawa, S.; Hayasaki, Y.; Mizeikis, V.; Buividas, R.; Juodkazis, S. Ultrafast laser processing of materials: from science to industry. *Light: Science & Applications* **2016**, *5*, e16133.
12. Kondic, L.; González, A.G.; Diez, J.A.; Fowlkes, J.D.; Rack, P. Liquid-State Dewetting of Pulsed-Laser-Heated Nanoscale Metal Films and Other Geometries. *Annual Review of Fluid Mechanics* **2019**, *52*, 2020.
13. Ruffino, F.; Grimaldi, M.G. Nanostructuration of Thin Metal Films by Pulsed Laser Irradiations: A Review. *Nanomaterials* **2019**, *9*, 1133.
14. Hale, G.M.; Querry, M.R. Optical constants of water in the 200-nm to 200-μm wavelength region. *Applied optics* **1973**, *12*, 555–563.
15. Hu, M.; Chen, J.; Li, Z.Y.; Au, L.; Hartland, G.V.; Li, X.; Marquez, M.; Xia, Y. Gold nanostructures: engineering their plasmonic properties for biomedical applications. *Chemical Society Reviews* **2006**, *35*, 1084–1094.
16. Pavlov, D.; Syubaev, S.; Kuchmizhak, A.; Gurbatov, S.; Vitrik, O.; Modin, E.; Kudryashov, S.; Wang, X.; Juodkazis, S.; Lapine, M. Direct laser printing of tunable IR resonant nanoantenna arrays. *Applied Surface Science* **2019**, *469*, 514–520.
17. Wang, X.W.; Kuchmizhak, A.A.; Li, X.; Juodkazis, S.; Vitrik, O.B.; Kulchin, Y.N.; Zhakhovsky, V.V.; Danilov, P.A.; Ionin, A.A.; Kudryashov, S.I.; Rudenko, A.A.; Inogamov, N.A. Laser-Induced Translative Hydrodynamic Mass Snapshots: Noninvasive Characterization and Predictive Modeling via Mapping at Nanoscale. *Physical Review Applied* **2017**, *8*, 044016.
18. Inogamov, N.A.; Zhakhovsky, V.V.; Khokhlov, V.A.; Petrov, Y.V.; Migdal, K.P. Solitary nanostructures produced by ultrashort laser pulse. *Nanoscale research letters* **2016**, *11*, 177.
19. Pavlov, D.; Gurbatov, S.; Kudryashov, S.; Danilov, P.; Porfirev, A.; Khonina, S.; Vitrik, O.; Kulinich, S.; Lapine, M.; Kuchmizhak, A. 10-million-elements-per-second printing of infrared-resonant plasmonic arrays by multiplexed laser pulses. *Optics Letters* **2019**, *44*, 283–286.
20. Nakata, Y.; Okada, T.; Maeda, M. Nano-sized hollow bump array generated by single femtosecond laser pulse. *Japanese Journal of Applied Physics* **2003**, *42*, L1452.
21. Matsuo, S.; Juodkazis, S.; Misawa, H. Femtosecond laser microfabrication of periodic structures using a microlens array. *Applied Physics A* **2005**, *80*, 683–685.
22. Kuchmizhak, A.; Porfirev, A.; Syubaev, S.; Danilov, P.; Ionin, A.; Vitrik, O.; Kulchin, Y.N.; Khonina, S.; Kudryashov, S. Multi-beam pulsed-laser patterning of plasmonic films using broadband diffractive optical elements. *Optics letters* **2017**, *42*, 2838–2841.
23. Aristov, A.I.; Zywietz, U.; Evlyukhin, A.B.; Reinhardt, C.; Chichkov, B.N.; Kabashin, A.V. Laser-ablative engineering of phase singularities in plasmonic metamaterial arrays for biosensing applications. *Applied Physics Letters* **2014**, *104*, 071101.
24. Kudryashov, S.; Danilov, P.; Porfirev, A.; Saraeva, I.; Nguyen, T.; Rudenko, A.; Khmelnitskii, R.; Zayarny, D.; Ionin, A.; Kuchmizhak, A.; others. High-throughput micropatterning of plasmonic surfaces by multiplexed femtosecond laser pulses for advanced IR-sensing applications. *Applied Surface Science* **2019**, *484*, 948–956.
25. Moutzouris, K.; Papamichael, M.; Betsis, S.C.; Stavrakas, I.; Hloupis, G.; Triantis, D. Refractive, dispersive and thermo-optic properties of twelve organic solvents in the visible and near-infrared. *Applied Physics B* **2014**, *116*, 617–622.

26. Kedenburg, S.; Vieweg, M.; Gissibl, T.; Giessen, H. Linear refractive index and absorption measurements of nonlinear optical liquids in the visible and near-infrared spectral region. *Optical Materials Express* **2012**, *2*, 1588–1611.
27. Anker, J.N.; Hall, W.P.; Lyandres, O.; Shah, N.C.; Zhao, J.; Van Duyne, R.P. Biosensing with plasmonic nanosensors. In *Nanoscience and Technology: A Collection of Reviews from Nature Journals*; World Scientific, 2010; pp. 308–319.
28. Pierce, D.; Spicer, W.E. Electronic structure of amorphous Si from photoemission and optical studies. *Physical Review B* **1972**, *5*, 3017.
29. Kischkat, J.; Peters, S.; Gruska, B.; Semtsiv, M.; Chashnikova, M.; Klinkmüller, M.; Fedosenko, O.; Machulik, S.; Aleksandrova, A.; Monastyrskyi, G.; others. Mid-infrared optical properties of thin films of aluminum oxide, titanium dioxide, silicon dioxide, aluminum nitride, and silicon nitride. *Applied optics* **2012**, *51*, 6789–6798.
30. Honda, M.; Ichikawa, Y.; Rozhin, A.G.; Kulinich, S.A. UV plasmonic device for sensing ethanol and acetone. *Applied Physics Express* **2018**, *11*, 012001.
31. Kuchmizhak, A.; Vitrik, O.; Kulchin, Y.; Storozhenko, D.; Mayor, A.; Mirochnik, A.; Makarov, S.; Milichko, V.; Kudryashov, S.; Zhakhovsky, V.; others. Laser printing of resonant plasmonic nanovoids. *Nanoscale* **2016**, *8*, 12352–12361.
32. Wang, X.; Kuchmizhak, A.; Storozhenko, D.; Makarov, S.; Juodkazis, S. Single-step laser plasmonic coloration of metal films. *ACS applied materials & interfaces* **2018**, *10*, 1422–1427.
33. Favier, F.; Walter, E.C.; Zach, M.P.; Benter, T.; Penner, R.M. Hydrogen sensors and switches from electrodeposited palladium mesowire arrays. *Science* **2001**, *293*, 2227–2231.
34. Liu, N.; Tang, M.L.; Hentschel, M.; Giessen, H.; Alivisatos, A.P. Nanoantenna-enhanced gas sensing in a single tailored nanofocus. *Nature materials* **2011**, *10*, 631.